Performance Comparison between Two Established Microgrid Planning MILP Methodologies Tested On 13 Microgrid Projects

Michael Stadler [1,2,3,4,*] , **Zack Pecenak** [1] , **Patrick Mathiesen** [1] , **Kelsey Fahy** [1] **and Jan Kleissl** [4]

1   Bankable Energy|XENDEE Inc., 6540 Lusk Blvd, San Diego, CA 92121, USA; ZPecenak@xendee.com (Z.P.); pmathiesen@xendee.com (P.M.); fahykt@xendee.com (K.F.)
2   Bioenergy and Sustainable Technologies Research GmbH, 3250 Wieselburg, Austria
3   Center for Energy and Innovative Technologies (CET), 3681 Hofamt Priel, Austria
4   Center for Energy Research, University of California at San Diego, 9500 Gilman Dr., San Diego, CA 92037, USA; jkleissl@eng.ucsd.edu
*   Correspondence: mstadler@xendee.com or mstadler@cet.or.at; Tel.: +1-619-431-1689

Abstract: Mixed Integer Linear Programming (MILP) optimization algorithms provide accurate and clear solutions for Microgrid and Distributed Energy Resources projects. Full-scale optimization approaches optimize all time-steps of data sets (e.g., 8760 time-step and higher resolutions), incurring extreme and unpredictable run-times, often prohibiting such approaches for effective Microgrid designs. To reduce run-times down-sampling approaches exist. Given that the literature evaluates the full-scale and down-sampling approaches only for limited numbers of case studies, there is a lack of a more comprehensive study involving multiple Microgrids. This paper closes this gap by comparing results and run-times of a full-scale 8760 h time-series MILP to a peak preserving day-type MILP for 13 real Microgrid projects. The day-type approach reduces the computational time between 85% and almost 100% (from 2 h computational time to less than 1 min). At the same time the day-type approach keeps the objective function (OF) differences below 1.5% for 77% of the Microgrids. The other cases show OF differences between 6% and 13%, which can be reduced to 1.5% or less by applying a two-stage hybrid approach that designs the Microgrid based on down-sampled data and then performs a full-scale dispatch algorithm. This two stage approach results in 20–99% run-time savings.

Keywords: Microgrid; DER; planning; MILP; optimization; run-time; full time-series optimization; data reduction; DER-CAM; XENDEE

1. Introduction

Microgrid deployment is accelerating rapidly and roughly 2300 Microgrids were operational or planned worldwide in 2018 [1]. In the last 6 months of 2018, 240 additional Microgrid projects were added to the Navigant database, demonstrating a steady increase in Microgrid projects. More impressive is the increase in 2019. As of June 2019, Navigant identifies 4475 Microgrid projects worldwide [2]. Microgrid Knowledge [3] estimates that the Microgrid market will reach US$31 billion by the year 2027, underscoring the need for effective, fast Microgrid design and planning tools to keep up with the increasing number of projects.

The research community provides several different methodologies to plan a Microgrid from an economic perspective. All methodologies need to match energy supply with Microgrid demand to determine the annual energy costs, Net Present Value (NPV), or emissions from Microgrid adoption. Investment costs, operation and maintenance costs, subsidies, tax incentives or carbon costs among

others are considered in this calculation [4]. The goal of these approaches is to determine the optimal combination of Distributed Energy Resources (DER) and their sizes to meet the demand, subject to constraints and inputs.

In simulation or trial and error approaches, the user changes input data (e.g., investment costs for DER) to analyze the impact on the results (e.g., adopted technologies in a Microgrid) [5]. While simulation approaches are helpful to understand a complex system by running multiple iterations in a manual fashion, simulation approaches do not have built-in mechanisms (i.e., mathematical solvers) to find the best or optimal solution (e.g., optimal DER capacity). Since there are often millions of combinations for technology choices and operational levels, simulation approaches can require enormous numbers of iterations to find the optimal technology combinations. Optimal operational dispatches (e.g., unit commitment for multiple DERs) are also elusive for simulation approaches, and will significantly increase runtimes. Fescioglu-Unver et al. [6] conclude that rule-based, i.e., assumption-based simulation approaches are not viable to guarantee optimal dispatch results; instead optimization techniques should be used to increase the profitability of Microgrids.

Mixed Integer Linear Programming (MILP) optimization algorithms and associated mathematical solvers can overcome the limitations of simulation approaches and deliver optimal economic and/or green house gas solutions in a single run, creating a viable path to identify the best DER portfolio and dispatch.

As indicated in [7] the process of designing a Microgrid, which comprises conceptual design, technical design, electrical analysis, power flow analysis, and implementation, can be very time consuming. Thus, any economic optimization algorithm attempting to deliver the optimal DER portfolio, lowest costs, and optimal dispatch must be fast while maintaining accuracy. Examples for such optimization tools are REopt [8] and DER-CAM [9]. These tools are already actively used in the Microgrid industry for real Microgrid design. Reopt uses a full-scale MILP approach optimizing each hour of the year explicitly while DER-CAM relies on a peak-preserving day-type approach to reduce run-times.

Other examples for economic Microgrid optimization algorithms can be found in [10–12]. A common challenge for these optimization algorithms is run-time, which ranges between 0.1 and 280 h, depending on the considered technologies in a Microgrid and optimization approach (see Figure 1). Each optimization approach using a full annual dataset of 8760 hourly data points exhibits run-times above 2.8 h, rendering such approaches impractical for real-world Microgrid design projects since dozen or even hundreds of sensitivity runs might be needed. [10,11] demonstrate that down-sampling the data to representative days can reduce the run-time below 1 h. However, down-sampling impacts on the objective function and technology adoption need to be analyzed for multiple Microgrid and DER projects. Schütz et al. in [11] perform a comparison for two test cases between an 8760 optimization and different k-means down-sampling approaches. Gabrielli et al. in [10] test different optimization methods to address the issue of discontinuity between representative periods when modeling seasonal storage in energy systems, but for only two test cases.
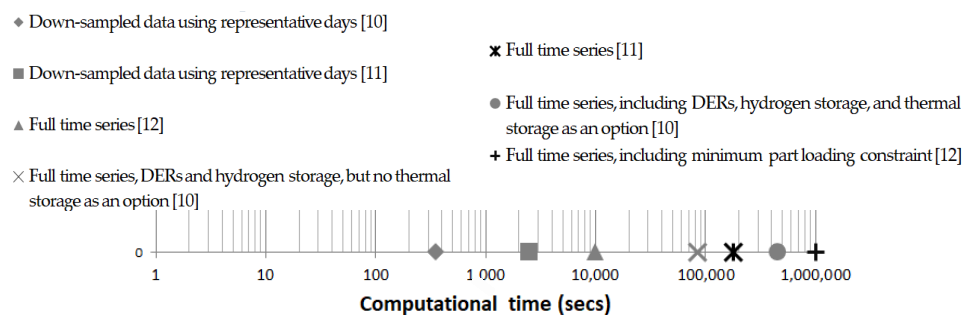
Figure 1. Run-time comparisons for different optimization approaches and use-cases. The different model setups tested in [10–12] result in considerable different run-times. The legend is ordered from small to large computational time. Please note the logarithmic scale.

Fahy et al. [13] demonstrate a peak load preserving down-sampling method and compare the technology selection as well as the Objective Function (OF) to a full-scale time-series optimization approach (FSO). For a single example, the results show OF differences below 1% and no technology adoption difference, but run-time savings of 90%. The authors of [13] also show that clustering with k-means always delivers worse OF results than the peak-preserving day-type approach selected for this study.

The literature review and our research indicate that traditional FSO approaches might be prohibitive for wide-spread Microgrid design, unless special hybrid optimization (HO) approaches are used. Typically, such HO approaches use two stages, in which the first stage optimizes the Microgrid technology adoption based on down-sampled representative day optimization (RO) [14]. Technology adoption results from the first stage are used to inform the second stage for dispatch optimization. Pecenak et al. [15] introduce a new HO approach that applies a minimum DER constraint, derived from the first HO stage, to the second stage. This approach also guarantees robust Microgrid outage modeling solutions by combining the peak preserving day-type approach with a FSO approach.

Down-sampling methodologies and HO approaches show great potential for industry applications, but an extensive performance comparison involving more than two test sites is lacking. Thus, this research compares the peak load preserving down-sampling RO approach from [13] and the FSO approach for 13 real Microgrid projects in the US. We address how the Microgrid setup and input data drive OF differences between the RO and FSO, as well as the impact of DER sizing deviations in the two models. Additionally, we research how the embedded MILP dispatch modeling of the second (dispatch) stage in an HO reduces the OF differences between RO and FSO.

2. Model Description and Used Data Down-Sampling

The mathematical optimization model has been documented in the literature numerous times and is based on the Distributed Energy Resources Customer Adoption Model (DER-CAM) [9]. Several studies have expanded on DER-CAM. Mashayekh et al. [16] added power flow and multi-node capabilities, allowing for optimal placement of DER technologies in a distribution network. To keep run-times low for such a power flow version the RO is needed. Cardoso et al. [17] describe an Ancillary Service market MILP extension for DER-CAM and show how such markets impact the Microgrid design. Milan et al. [18] introduce nonlinear efficiency modeling for CHP systems and describe the MILP in detail. Especially the modelling of nonlinear behavior increases the run-times considerably and call for RO approaches. A DER-CAM version with considerations of passive building measures is established in [19], which allows DER and building technology optimization to create zero carbon solutions. Another version considers electric vehicle (EV) modeling under uncertainty [20] and has been applied to assess the impact of EV interconnections on optimal DER solutions. The authors of [21] consider outage modeling in DER-CAM by adding a particle swarm optimization to determine the optimal investment and operation of DER equipment. Solar variability has been incorporated by [22] and the impact on Microgrid design has been studied. The most recent version of DER-CAM implements also an efficient multi-year optimization [23] based on a RO. In this paper we use DER-CAM, implemented in XENDEE [24], as basis for the peak load preserving down-sampling RO runs for the 13 Microgrid projects.

The process of solving the MILP based on Figure 2 can be very time consuming since the amount (represented as arrow width) of each energy flow is not static over the modeled time horizon, but can change considerably with each time-step, because of, e.g., available solar radiation or changes in electric rates. Solving such a MILP with full time-series data sets, each containing 8760 data points for hourly resolution or 35,040 for 15 min resolution (or even more data points in a multi-year setting), can take hundreds of hours. Thus, down-sampling methodologies are used to reduce the run-time. We refer to this down-sampling representative day optimization as RO.
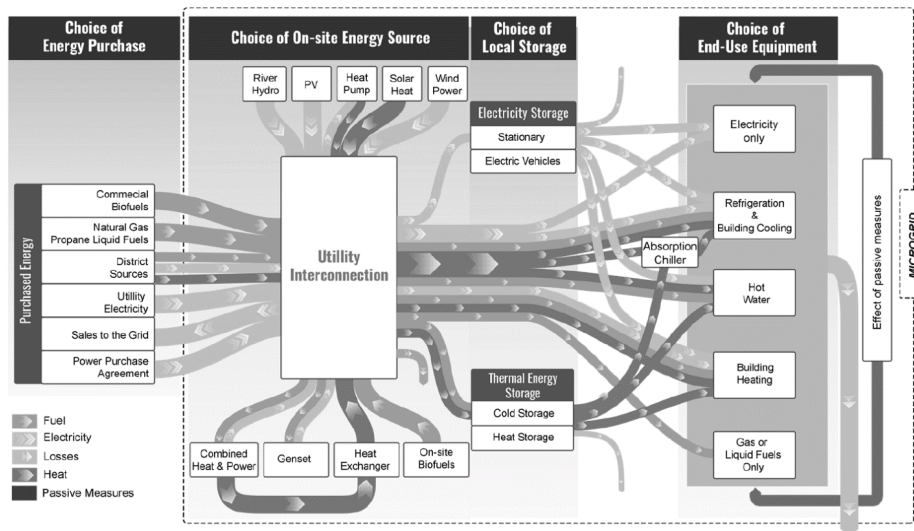
Figure 2. Sankey diagram for the Microgrid DER-CAM/XENDEE MILP. The five energy end-uses on the right hand side need to be supplied with energy at minimized annual energy costs or CO_2 emissions. The MILP analyzes the energy flows (different arrows) in each time-step and decides on the optimal investment capacities and technologies as well as energy flows in each time-step, constituting an optimal dispatch profile.

2.1. Peak Preserving Day-Types Representative Optimization (RO)

The peak preserving RO is a special data reduction method that preserves both total annual energy demand and demand peaks. The peak preserving approach reduces annual hourly demand data into typical weekday and weekend profiles as well as peak demand day profiles. For each month m, one 24 h profile of each day-type is constructed with an hourly resolution. The total annual energy consumption is calculated using multipliers to scale up typical weekday, weekend, and peak demand day-type profiles, with the multipliers ND representing the number of times each day-type d occurs in a given month m ($ND_{m,d}$).

The peak demand day profile for each month is constructed by selecting at each hour the maximum demand across any given day in the month. The resulting peak day profile represents both peak daily consumption and peak monthly demand. An example of the peak demand profile is shown in Figure 3.
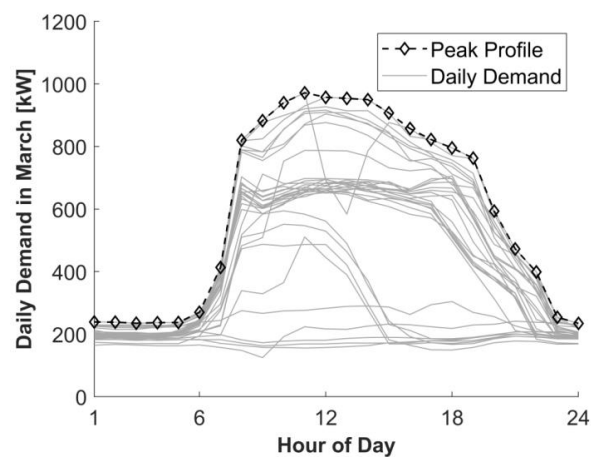
Figure 3. Daily demand for each day in an example March month and peak demand day profile constructed from selecting maximum hourly demand across all days.

The representative weekday and weekend demand profiles must both represent the average weekday and weekend demand behavior, while also maintaining the monthly total energy consumption.

Therefore, the average weekday and weekend profiles are adjusted to account for the energy contained in the peak demand profiles. The monthly demand data are separated into sets of weekday and weekend data. The sets are summed to calculate the total weekday demand and weekend demand for each hour in the day. The total weekday demand data for month m is modified by subtracting the peak demand, multiplied by the number of peak days expected to occur in the month, from the weekday consumption at each hour the peak occurred on a weekday. As indicated by [13] the number of peak days is not crucial and just using one peak day profile in the optimization is sufficient. The same approach is used to modify the weekend consumption data, based on peaks occurring on weekends. The modified total weekday and weekend demand data sets are averaged into 24-h representative weekday and weekend demand profiles.

RO MILP

The energy end-uses (u) are grouped into three characteristic groups d: weekdays, weekend days, and peak days for each month. The MILP approach is solved for the entire year, resulting in 36 daily profiles and 864 hourly data points. A brief overview of the MILP is given in what follows and additional selected constraints are given in Figure 4.

The objective function minimizes the total costs C

$$
\begin{aligned}
= & \sum_m \mathrm{MFix_m} + \sum_{u,m,d,h} u\, \widetilde{~}_{u,m,d,h} \cdot \mathrm{C_{u,m,d,h}} \cdot \mathrm{ND_{m,d}} \\
& + \sum_{u,m,p} \max u\, \widetilde{~}\widetilde{~}_{u,p,m} \cdot \mathrm{D_{u,p,m}} \\
& + \sum_g num_g \cdot \mathrm{IFix_g} \cdot \mathrm{ANN_g} + \sum_{c \cup s} (pur_{c \cup s} \cdot \mathrm{IFix_{c \cup s}} + cap_{c \cup s} \cdot \mathrm{IVar_{c \cup s}}) \cdot \mathrm{ANN_{c \cup s}} \\
& + \sum_{j,u,m,d,h} \frac{gen_{j,u,m,d,h}}{\eta_j} \cdot \mathrm{GENC_{j,u,m,d,h}} \cdot \mathrm{ND_{m,d}} + \sum_{u,m,d,h} dr_{u,m,d,h} \cdot \mathrm{DRC_{u,m,d,h}} \cdot \mathrm{ND_{m,d}} \\
& - \sum_{i,m,d,h} sell_{i,m,d,h} \cdot \mathrm{S_{m,d,h}} \cdot \mathrm{ND_{m,d}}
\end{aligned}
\tag{1}
$$

Major constraint Energy Balance :

$$
\begin{aligned}
& \sum_{u,m,d,h} \mathrm{LOAD_{u,m,d,h}} + \sum_{i,m,d,h} sell_{i,m,d,h} + \sum_{s,m,d,h} sin_{s,m,d,h} + \sum_{u,m,d,h} dr_{u,m,d,h} \\
& = \sum_{u,m,d,h} u\, \widetilde{~}_{u,m,d,h} + \sum_{i,u,m,d,h} gen_{i,u,m,d,h} + \sum_{s,u,m,d,h} sout_{s,u,m,d,h}
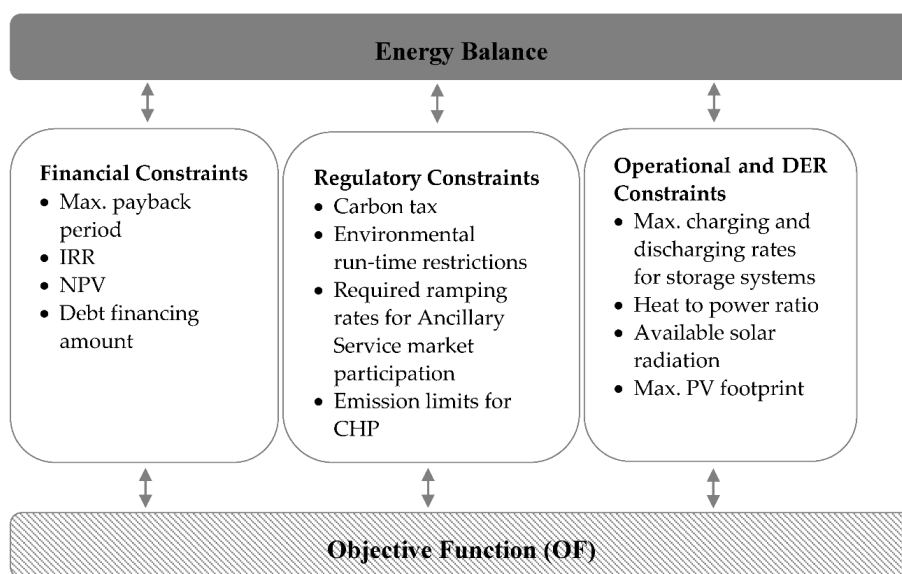\end{aligned}
\tag{2}
$$

Energy Balance

Financial Constraints
- Max. payback period
- IRR
- NPV
- Debt financing amount

Regulatory Constraints
- Carbon tax
- Environmental run-time restrictions
- Required ramping rates for Ancillary Service market participation
- Emission limits for CHP

Operational and DER Constraints
- Max. charging and discharging rates for storage systems
- Heat to power ratio
- Available solar radiation
- Max. PV footprint

Objective Function (OF)

Figure 4. Selected constraints of the MILP.

Indices

c	continuous generation technologies (assumed to be available in any size), c ∈ **C** = {photovoltaic panels, solar thermal panels, and absorption chillers}
d	day-types, d ∈ **D** = {week, peak, weekend}
g	discrete generation technologies (explicitly modeled in discrete sizes), internal combustion engines (ICE), micro turbines (MT), fuel cells (FC), and gas turbines (GT), with and without heat exchangers (HX), g ∈ **G** = {ICE, ICEHX, MT, MTHX, FC, FCHX, GT, GTHX}. All discrete technologies without HX are referred to as DG, DG with HX as CHP
h	hours in a day h ∈ **H** = {1, 2, . . . , 24}
i	DER technologies, i ∈ **I** = **J** ∪ **S**
j	generation technologies, j ∈ **J** = **G** ∪ **C**
m	months in a year, m ∈ **M** = {1, 2, . . . , 12}
p	utility demand periods, p ∈ **P** = {coincident, on peak, mid peak, off peak}
s	energy storage technologies, stationary storage and heat storage, s ∈ **S** = {electric energy storage systems, heat storage}
u	energy end-uses for each day-type (d), including electricity-only (eo), cooling (cl), space heating (sh), water heating (wh), and natural gas loads (ng), u ∈ **U** = {eo, cl, sh, wh, ng}

Parameters

ANN_i	annuity rate of investing in DER technology i
$ND_{m,d}$	number of days of type d in month m
$C_{u,m,d,h}$	volumetric electricity charges
$D_{u,p,m}$	charges applied to peak power demand for end-use u during period p, and month m
$DRC_{u,m,d,h}$	volumetric demand response costs
$GENC_{j,u,m,d,h}$	fuel costs, maintenance costs
$IFix_i$	fixed investment cost of DER technology i
$IVar_{c \cup s}$	variable investment cost of continuous energy conversion technology c, or storage technology s
$LOAD_{u,m,d,h}$	Microgrid energy demand for end-use u, in month m, day-type d, and hour h
$MFix_m$	fixed monthly utility charges/contract demand charges
$S_{m,d,h}$	electricity sales price in month m, day-type d, and hour h
η_i	energy conversion efficiency for i

Decision Variables

$cap_{c \cup s}$	installed capacity of continuous generation technology c, or storage technology s
$dr_{u,m,d,h}$	energy demand of end-use u removed by demand response measures in month m, day d, and hour h
$gen_{j,u,m,d,h}$	useful (e.g., electric output) energy provided by generation technology j for end-use u in month m, day-type d, and hour h
num_g	number of installed units of discrete generation technology g
$pur_{c \cup s}$	binary purchase decision for continuous generation technology c, or storage technology s
$sell_{i,u,m,d,h}$	energy sales from technology i that is exported in month m, day-type d, and hour h
$sin_{s,m,d,h}$	energy input to storage technology s, in month m, day-type d, and hour h
$sout_{s,u,m,d,h}$	energy output from storage technology s for end-use u, in month m, day-type d, and hour h
$u \sim_{u,m,d,h}$	utility purchase for end-use u, during month m, day-type d, and hour h

2.2. Full-Scale Time-Series Optimization (FSO)

Since DER-CAM was programmed as a RO model, the FSO requires some adjustment of the day-type framework to emulate an FSO. The FSO MILP model is derived from the RO model by modifying $ND_{m,d}$ to represent the real number of days in a month instead of the number of representative day-types. Thus, instead of e.g., using 22 representative weekdays, eight weekend days, and one peak profile for the RO, we convert $ND_{m,d}$ into a binary matrix containing ones to identify the real days observed in each month. In the case of January 2020, the matrix consists of ones from 1 to 31. For February 2020 it consists of ones from 1 to 29 and zeros for 30 and 31, etc. Days must be linked in

time to allow energy to shift between consecutive days, creating a real seasonal model. The authors of [15] describe the changes needed to create an FSO model in detail.

Additionally, we link the RO and FSO to create a Hybrid Optimization (HO) approach. In such an HO approach the sizing (e.g., DER capacity) solution from the down-sampled RO will be used as fixed input for the FSO. In other words, the FSO just optimizes the dispatch of the RO-designed Microgrid using the full time-series data which preserves short run-times. To differentiate between a real FSO, which also sizes DERs, and the full time-series dispatch optimization within the HO, we call the latter TSO. The second part of this paper will compare the OF and run-time results of a simple RO with those of an HO, utilizing a TSO as a second stage.

3. Microgrid Projects

### 3.1. General Description of Microgrid Projects

Table 1 presents an overview of the Microgrid projects. Cases were selected to represent a diverse variety of host types, geographic locations, tariff characteristics, and total load consumption. These Microgrid projects have been modeled by the authors in detail. All the projects are optimized using the RO, FSO, and HO models, and results are assessed from an economic perspective.

All Microgrids are grid connected without grid outages considered, except for Mil2, for which we modeled a 24-h outage on the day with the highest electric peak demand, which in this case constitutes also the highest daily energy consumption. None of the Microgrids are allowed to sell electricity to the utility, except for Un1, which is on a net-metering tariff and can export surplus electricity to the utility. To analyze effects of electricity sales we will show hypothetical sensitivity runs for selected sites in Section 4.2.

The tariffs and technology data are summarized in the Appendices A and B.

3.2. Electric Load Data

For each case except Un4, hourly metered load data for one year was used in this analysis (8760 data points per case for FSO and HO). In the absence of metered load data, for Un4, data from the Commercial and Residential Hourly Load Profile database for a hospital was used since the modeled site is a medical University [25]. Segments of the time-series electric load data for Un3 and Un4 are provided in Figure 5.
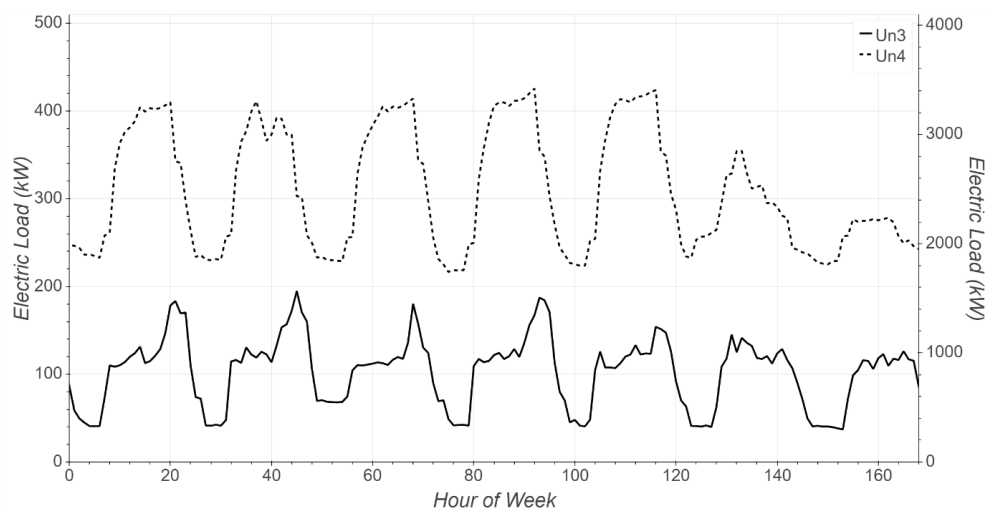

Figure 5. Example time-series electric load data for Un3 (solid line, left *y*-axis) and Un4 (dashed line, right *y*-axis). Hours 120–168 are weekend days.

Table 1. Overview of considered Microgrid projects for this research. FER: Flat energy rate, FSER: Flat seasonal energy rate, FER-winter: Flat energy rate just for winter months, TOUER: Time-Of-Use energy rate, TOUER-summer: Time-Of-Use energy rate just for summer months, NCDC: Non-coincident demand charge, PDC: Peak demand charge, MPDC: Mid peak demand charge. PV: Photovoltaics, EES: Electric Energy Storage, CHP: Combined Heat and Power, DG: Distributed Generation as natural gas or diesel fired backup systems. All Microgrid projects are in the US, due to confidentiality reasons the exact locations cannot be revealed.

Case	Type	State/Territory	Techn. Modeled	Tariff Characteristics	Annual Electrical Cons. (MWh)	Annual Heating Cons. (MWh)	Electric Peak Load (MW)
Ind	Industrial/Pharmaceutical	Puerto Rico	PV, EES	FER, NCDC, PDC, MPDC	22,642	n/a	3.96
Res	Residential/Public	Connecticut	PV, EES, DG	TOUER, NCDC	1640	n/a	0.37
Man	Industrial/Materials	Puerto Rico	PV, EES, CHP	FER, NCDC	78,400	41,854	12.48
Com	Commercial/Public	Washington State	PV, EES, CHP	FER, NCDC	4263	667	0.93
Un1	University	Colorado	PV, EES, DG	TOUER-summer, FER-winter, PDC	12,076	n/a	2.85
Un2	University	Hawai'i	PV, EES	FER, NCDC	3338	n/a	0.97
Un3	University	California	PV, EES, DG	TOUER, NCDC, PDC	825	n/a	0.20
Un4	University	Vermont	PV, EES, DG	FER, NCDC	26,713	6817	5.00
Mil1	Military	Texas	PV, EES, DG	TOUER, NCDC	330,648	n/a	67.61
Mil2	Military	New Mexico	PV, EES, DG	TOUER, NCDC	78,878	n/a	15.99
Mil3	Military	Maryland	PV, EES, DG	FSER, NCDC	187,645	n/a	33.96
Mil4	Military	California	PV, EES, DG	TOUER, NCDC	86,349	n/a	15.00
Mil5	Military	Massachusetts	PV, EES, DG	TOUER, NCDC	16,564	n/a	3.41

Figure 6 summarizes the electric load data statistics. Total annual electric load is the sum of the hourly electric load profile over the entire year. Annual load variability is the sum of the absolute value of hourly energy ramp rates (ERR_n) normalized by the total annual electric load to ensure that load volatilities can be compared between sites (Equation (3)).

$$Annual\ Load\ Variability = \frac{\Sigma(abs(ERR_n))}{\Sigma_{m,d,h}load_{m,d,h}} = \sum_{m,d,h}\frac{load_{m,d,h} - load_{m,d,h-1}}{\Sigma_{m,d,h}load_{m,d,h}} \tag{3}$$
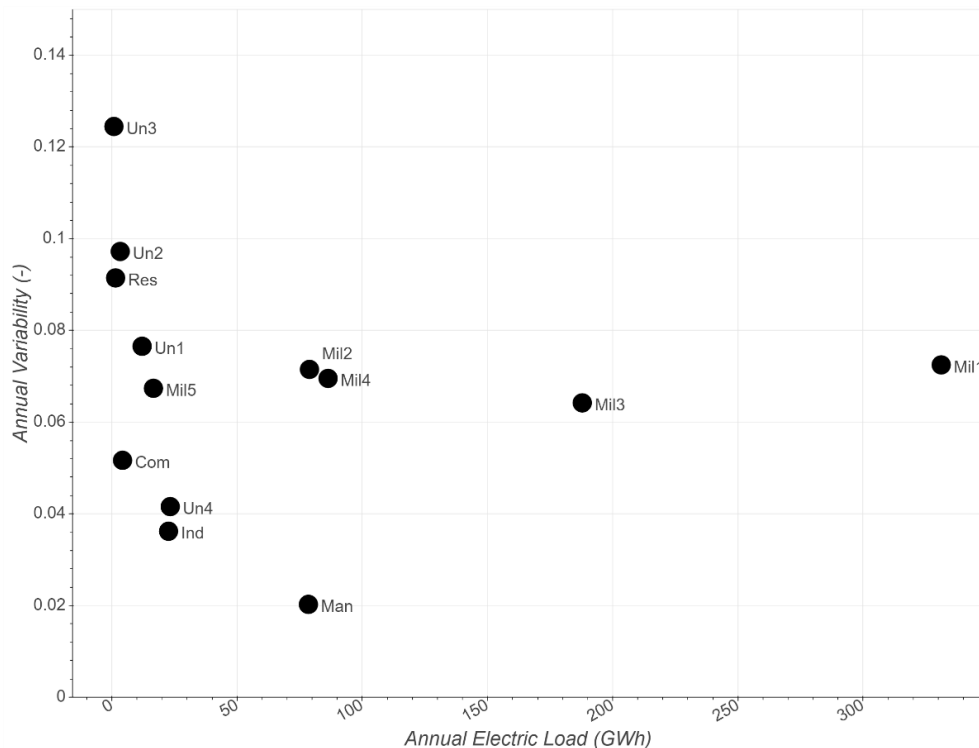
Figure 6. Summary of electric load data for all cases as a function of annual electric load (GWh) and load variability (-) expressed as the sum of the absolute values of all 1 h power changes normalized by the total annual load.

For example, the Un3 metered data is more volatile, with severe late afternoon ramps and a total variability equal to 12.4% of its annual load. Un4, on the other hand, is relatively smooth, and therefore, shows low variability numbers of 4.2% in Figure 6, which also can be attributed to the load modeling. Overall, the two industrial sites (Ind and Man) have the lowest variability. The military sites Mil1 and Mil3 have significantly larger annual loads than the other cases.

3.3. Solar Radiation Data

Several sources of solar radiation data were used for the different Microgrid projects as input for the RO, FSO, and TSO MILP: real measurements of solar radiation (two projects), Helioscope [26] data (six projects), and PVWatts data based on the NREL National Solar Radiation Database from satellite data (NSRDB, five projects) [27]. While the FSO and TSO use the 8760 PV Watts output directly, the RO uses an average daily profile for each month constructed from the 8760 time-series.

Similar to Figure 6, Figure 7 compares the solar production data across all sites via the capacity factors and total variability. Similar to the demand, total solar variability is calculated by summing

over the absolute values of solar production ramp rates (SRR_n) and normalizing them by the total energy production (Equation (4)).

$$Annual\ Solar\ Variability = \frac{\Sigma(abs(SRR_n))}{\Sigma_{m,d,h}PV_{m,d,h}} = \sum_{m,d,h} \frac{PV_{m,d,h} - PV_{m,d,h-1}}{\Sigma_{m,d,h}PV_{m,d,h}} \tag{4}$$
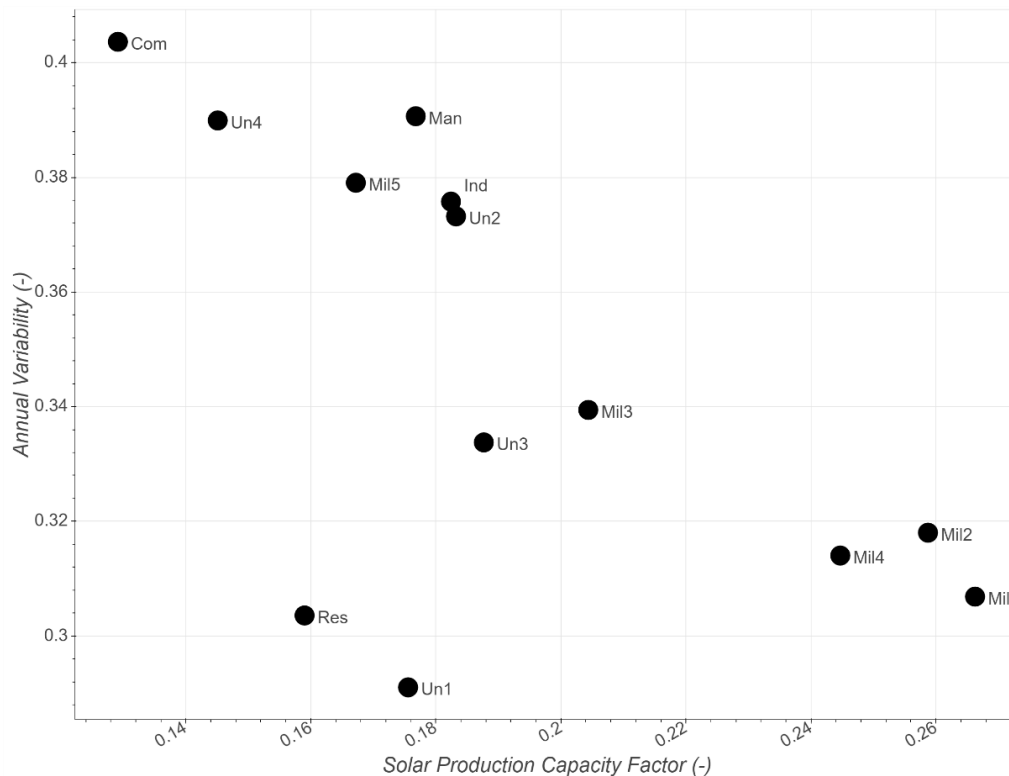
Figure 7. Solar production summary for all cases expressed through the annual capacity factor and the normalized annual solar variability.

Figure 7 is useful to infer case-by-case differences in the solar resource. For example, Mil1, Mil2, and Mil4 are located in sunny locations with little variability due to clouds. As such, variability is low and total solar production and capacity factors are high. Conversely, Com is in a region with low total solar production and high variability, indicating frequent cloud cover and ramp events.

4. Results

4.1. Representative Optimization (RO) versus Full-Scale Time-Series Optimization (FSO)

Table 2, Figures 8 and 9 present the high level results for all 13 Microgrid cases, comparing the objective functions of RO and FSO, technology adoptions, and run-times. The run-time savings for the analyzed cases can range between almost 100% and 85%.

In total, 10 cases out of the 13 show OF differences below 1.5%. Un4, with a very high solar variability (see Figure 7) and small load variability shows the highest OF difference. This could explain the 97.4% difference in PV adoption between the RO and FSO. Some cases show very similar OFs for the RO and FSO models despite significant changes in the technology adoption, which is expected for MILP approaches. Examples are the Ind case with a −32% difference in EES adoption, but only a −0.5% OF difference or the Res case with a 56.9% difference in EES adoption, but only a −0.3% difference in the OF (see also Figure 9).
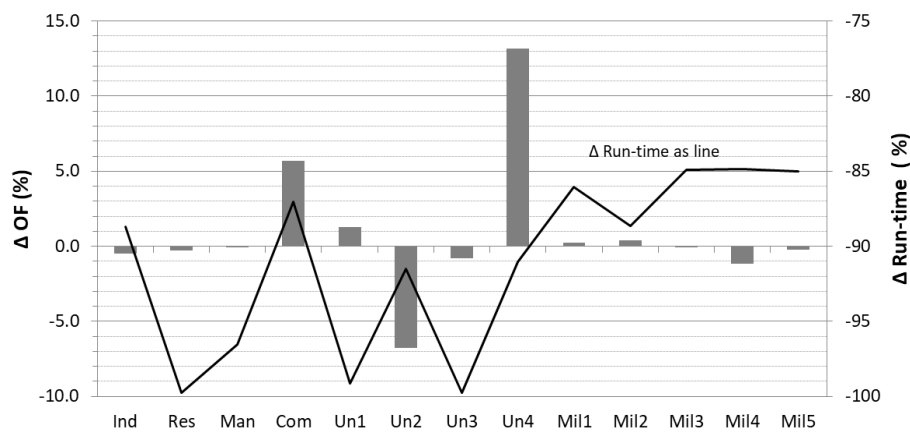
Figure 8. OF differences (bars) and run-time savings (line) for the RO approach compared to the FSO. Negative run-time numbers represent savings.
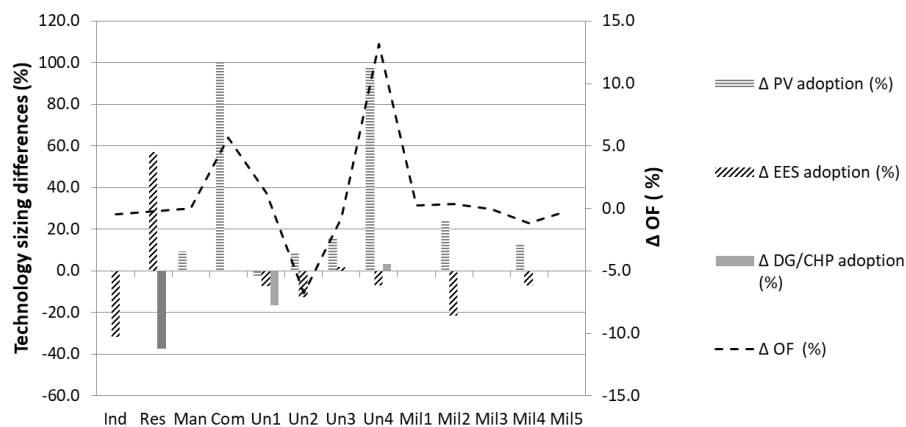
Figure 9. Variations in RO technology adoption compared to the FSO. The OF difference compared to FSO is shown as a dashed line.

It is worth noting that the Ind and Res cases experience opposite solar and load volatilities: Ind has a relative high solar variability compared to the Res case (see Figure 7) and a small load variability compared to the Res case (see Figure 6). Note that in the Ind and Res case the available PV space is fully utilized, explaining the exact same PV sizes in both optimization models.

Un3 with the highest load variability experiences one of the highest run-time savings between the two MILP models (99.8%), a very low OF difference of −0.8%, moderate PV difference (16%), very small EES differences (2%), and no difference in fuel fired DG adoption.

The Mil2 includes a 24 h outage and the possibility to install DG units. Since the RO model preserves the peak loads from the full time-series load data and the DG units contribute to the worst case outage modeling (highest power demand and electric energy consumption in a day in this case), the installed fuel fired DG units in the FSO and RO model match. The differences in the PV (24.3%) and EES (−21.4%) adoptions are influenced by the different granularity of the solar radiation modeling in the RO and FSO—the RO uses an average monthly solar production profile, while the FSO uses the full-scale time-series. However, the OF (e.g., project cost) differs by only 0.4%.

Com and Un4 show significant OF differences with higher costs in the RO model (i.e., ΔOF >0), which creates a budget cushion for these projects when modeled with RO, but could also render these projects economically unattractive. Their technology selection in the RO is higher except for the smaller EES numbers in the RO model for Un4 (Figure 9). Un2, on the other hand, shows significant lower costs in the RO model, indicating that there is no clear trend on whether the RO is over- or underestimating OFs.

Figure 9 also shows that if sizing of several technologies differ for a Microgrid (seven cases), then RO oversizing of one technology is usually balanced by undersizing of another. In four of those seven cases RO oversizes PV and undersizes storage compared to the FSO, indicating that the technologies could be to some extent interchangeable.

Among these 13 Microgrid designs, there is no clear relationship between the solar variability and the deviation in the OF solution (Figure 10). Com, Un4, and Un2 tend to have higher solar variability and are the three cases which exhibit OF deviations greater than 1.5%. However, sites Man, Ind, and Mil5 also have high solar variability and small OF differences. However, for Mil5 no DER investments are optimal and installed. On the other hand, the load variability seems to have no significant impact on the OF differences, indicating that the peak-preserving down-sampling is an effective method to capture load spikes.
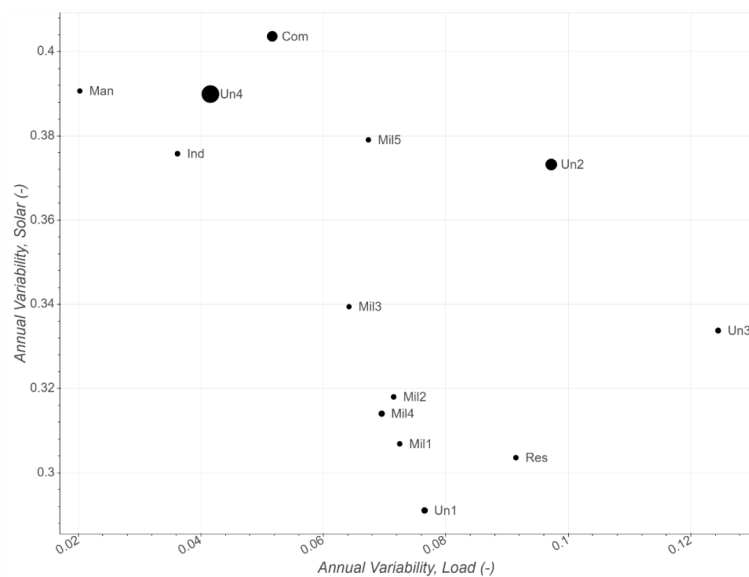
Figure 10. Scatter plot comparing the absolute value of OF deviation of each case as a function of solar variability (*y*-axis) and load variability (*x*-axis). The size of the circle represents the OF deviation of each case.

4.2. Sensitivity to Electricity Sales

A limitation of the Microgrid projects is that only site Un1 is explicitly considering energy sales to the utility, which inherently limits the economic viability and sizing for DERs, especially for solar PV. Thus, sensitivity scenarios are performed to assess the impact of electricity sales on OF differences as well as DER technology selections. For these sensitivities, two cases were selected, one with a minor OF difference of −1.2% (Mil4) and one with a considerable difference of −6.8% (Un2). These sites are representative as universities and military sites are prime Microgrid candidates considering their abundance in the set of real Microgrid projects in Table 1.

The sales prices are assumed to be the same as the energy purchase prices from the utility during the same time period. Capacity bidding or Ancillary Service market participation is not considered.

For the Un2 case, including energy sales the OF difference is reduced to −2.0% (see column 1 in Table 3 for the Un2 cases). In this particular case, the OF deviation reduction may be explained by identical PV capacity investments. When sales are considered, PV is attractive enough that both algorithms invest in PV to its spatial limit. However, the Un2 sales with FSO case shows less EES, which causes the Microgrid to import and export more energy on an annual basis compared to the RO approach (see Table 4 cells Un2 sales/A/B/D/E).

Table 2. Overview results for the 13 modeled Microgrids. OF: Objective Function; R-time: Run-time; RO: Down-sampled representative day-types optimization.

Case	1	2	3	4	5	6	7	8	9	10	11	12	13
	Δ OF (%)	R-Time RO (mins)	R-Time FSO (mins)	Δ R-Time (%)	PV RO (kW)	PV FSO (kW)	Δ PV Compared to FSO (%)	EES RO (kWh)	EES FSO (kWh)	Δ EES Compared to FSO (%)	DG/CHP RO (kW)	DG/CHP FSO (kW)	Δ DG/CHP Compared to FSO (%)
Ind	−0.5	0.2	1.6	−89	1568	1568	0.0	396	582	−32.0	0	0	n/a
Res	−0.3	0.3	121.0	−100	715	715	0.0	1048	668	56.9	100	160	−37.5
Man	0.0	0.3	7.4	−97	358	328	9.1	0	0	n/a	9975	9975	0
Com	5.7	0.2	1.7	−87	182	0	100.0 *)	0	0	n/a	0	0	n/a
Un1	1.3	1.0	121.1	−99	8969	9211	−2.6	8243	8909	−7.5	500	600	−16.7
Un2	−6.8	0.0	0.5	−92	1627	1501	8.4	2242	2573	−12.9	0	0	n/a
Un3	−0.8	0.2	88.5	−100	257	222	15.8	320	314	1.9	100	100	0
Un4	13.2	0.2	2.4	−91	995	504	97.4	2227	2400	−7.2	3000	2900	3.4
Mil1	0.3	0.2	1.5	−86	0	0	n/a	0	0	n/a	0	0	n/a
Mil2	0.4	0.3	2.2	−89	6107	4913	24.3	6600	8400	−21.4	12,000	12,000	0
Mil3	−0.1	0.2	1.4	−85	0	0	n/a	0	0	n/a	0	0	n/a
Mil4	−1.2	0.2	1.2	−85	13,053	11,600	12.5	7800	8400	−7.1	0	0	n/a
Mil5	−0.2	0.2	1.1	−85	0	0	n/a	0	0	n/a	0	0	n/a

*) Differences (Δ) are calculated as (RO data-FSO data)/FSO data, except for Δ PV adoption compared to the FSO approach to avoid an undefined in the Com case. Only in this case we use (RO data-FSO data)/RO data.

Table 3. Overview results for the sensitivity runs considering energy sales to the utility. OF: Objective Function; R-time: Run-time; RO: Representative Optimization approach; FSO: Full Scale Time-Series Optimization.

Case	1	2	3	4	5	6	7	8	9	10	11	12	13
	Δ OF (%)	R-Time RO (mins)	R-Time FSO (mins)	Δ R-Time (%)	PV RO (kW)	PV FSO (kW)	Δ PV Compared to FSO (%)	EES RO (kWh)	EES FSO (kWh)	Δ EES Compared to FSO (%)	DG/CHP RO (kW)	DG/CHP 8FSO (kW)	Δ DG/CHP Compared to FSO (%)
Un2 no sales	−6.8	0.0	0.5	−92	1627	1501	8.4	2242	2573	−12.9	0	0	n/a
Un2 sales	−2.0	0.0	0.6	−92	2994 *)	2994 *)	0	1412	1358	4	0	0	n/a
Mil4 no sales	−1.2	0.2	1.2	−85	13,053	11,600	12.5	7800	8400	−7.1	0	0	n/a
Mil4 sales	−1.1	0.1	0.8	−88	18,945	16,856	12.4	9000	9600	−6.3	0	0	n/a

*) In the Un2 case with sales the PV adoption is reaching the maximum available space at the site.

The Mil4 sales case does not show significant changes compared to the case without sales. The OF differences change from −1.2% to −1.1% and the PV/EES adoptions show slightly smaller differences compared to the Mil4 no sales case (see Table 4).

However, as indicated by Mil4 sales in Table 4, reduced differences in the technology adoption do not necessarily lead to a reduced difference in the imported energy. For Mil4, Δ PV changes from −12.5% to −12.4% and Δ EES from −7.1% to −6.3%, but Δ import decreases from −5.2% to −7.2% (Table 4).

These results underscore the complexity of such modelling problems and that similar technology adoption capacities can result in similar OFs, but different parts of the result can change in different directions.

Table 4. Import and export balance for the energy sale sensitivity runs as well as the original runs without sales.

Case	A	B	C	D	E	F
	Annual Export RO (MWh)	Annual Export FSO (MWh)	Δ Export Compared to FSO (%)	Annual Import RO (MWh)	Annual Import FSO (MWh)	Δ Import Compared to FSO (%)
Un2 no sales	0	0	n/a	962	1237	−22.2
Un2 sales	2720	2801	−2.9	1276	1366	−6.6
Mil4 no sales	0	0	n/a	58,694	61,920	−5.2
Mil4 sales	5088	4456	14.2	5138	5538	−7.2

4.3. The Influence of Optimal Dispatch Modeling—The Hybrid Optimization (HO)

The large OF differences for Com and Un4 and the connection to extreme relative capacity deviations will be analyzed.

In both Com and Un4, RO modeling delivers higher optimal capacities of PV and DG/CHP. In particular, the RO almost doubles the PV capacity for Un4 and invests in 182 kW of PV for Com, while FSO does not select any PV in Com. Only the optimal EES in the Un4 FSO is slightly higher than for the RO. We hypothesize that the OF differences resulting from large capacity deviations in the RO can be mitigated by dispatch optimization. To test this, optimal dispatch modeling in the FSO, based on optimal capacities from the RO, is performed. This approach constitutes a two stage Hybrid Optimization (HO) approach, in which we refer to the FSO as TSO to indicate that the full-scale time-series optimization of the second state will optimize the operational planning (i.e., dispatch), but not the capacities. The HO approach allows assessing the impact of dispatch on the OF differences. Additionally, the HO allows assessing the feasibility of a Microgrid designed by an RO when modeled using raw time-series data.

Taking the optimal investment capacity results from the RO and fixing them in the TSO model while allowing for dispatch optimization, yields OFs that are very similar to the FSO, but with better run-times as indicated in Table 5. The Com RO case shows a 5.7% OF deviation compared to the FSO OF. Using the 2-stage HO process with TSO reduces the deviation to 1.4%. Similarly, the Un4 RO deviation of 13.2% is reduced to a 0.6% difference with HO. Every other case also shows a reduction in the OF difference compared to the FSO with better run-times than the FSO.

These results are important for Microgrid planning and operation since they indicate that even though there occasionally are higher deviations between RO and FSO capacity results, the fast HO is very viable and will result in a similar OF as the slower FSO. The unit dispatch optimization absorbs OF deviations that arise from differences in the capacities between the models. Note that the TSO dispatch optimization in the HO is similar to dispatch modeling in real Microgrids through Model Predictive Controllers (MPC). Thus, actual Microgrid dispatch is economically robust (i.e., will achieve similar revenues and costs) to capacity differences introduced by sub-optimal RO modeling during Microgrid planning.

Table 5. Objective function as well as run-time differences between the HO and FSO. OF: Objective Function; R-time: Run-time; RO: Representative Optimization; HO: Hybrid Optimization; FSO: Full-Scale Time-Series Optimization.

Case	1	1a	2	2a	3	4	4a
	Δ OF RO Versus FSO (%)	Δ OF HO Versus FSO (%)	R-Time RO (mins)	R-Time HO (mins)	R-Time FSO (mins)	Δ R-Time RO Versus FSO (%)	Δ R-Time HO Versus FSO (%)
Com	5.7	1.4	0.2	0.9	1.7	−87	−48
Un4	13.2	0.6	0.2	1.0	2.4	−91	−58
Ind	−0.5	0.0	0.2	1.0	1.6	−89	−40
Res	−0.3	0.3	0.3	1.1	121.0	−100	−99
Man	0.0	0.0	0.3	1.0	7.4	−97	−87
Un1	1.3	0.2	1.0	1.8	121.1	−99	−98
Un2	−6.8	0.8	0.0	0.3	0.4	−92	−23
Un3	−0.8	0.7	0.2	1.1	88.5	−100	−99
Mil1	0.3	0.0	0.2	1.2	1.5	−86	−25
Mil2	0.4	0.3	0.3	1.1	2.2	−89	−50
Mil3	−0.1	0.0	0.2	0.9	1.4	−85	−34
Mil4	−1.2	0.3	0.2	0.9	1.2	−85	−27
Mil5	−0.2	0.0	0.2	0.9	1.1	−85	−20

5. Conclusions

This paper advances the field of Microgrid planning and operation through a comprehensive analysis of objective function and technology adoption results of peak preserving day-types Representative Optimization (RO). Not only does the analysis include a large number of Microgrids (13) with different load and renewable resource time-series, but also a great diversity of tariffs and technology assumptions. The uniqueness of the paper also stems from industry relevance in that the Microgrids are actually being considered for construction or are already being built and were analyzed in commercial applications.

The results support the widespread application of RO in Microgrid planning. The special peak-preserving day types approach represents a full time-series of 8760 h with 3 days in each month or 864 time-steps. For all but three Microgrids the objective function differences are less than 1.5%, yet run-time savings are from 85% to almost 100% compared to full-scale time-series optimization (FSO). Such run-time savings enable more detailed analysis through sensitivity studies, probabilistic parameter inputs (Monte Carlo Simulation) and decision-making, and multi-year horizon analysis.

Three analyzed Microgrids have larger OF differences at 5.7%, −6.8%, and 13.2% in the RO. All these outliers experience higher solar variability than others. However, three other Microgrids with similar or even higher solar variability experience very small OF differences of 0.0%, −0.2%, and −0.5%, indicating that there is no clear trend on how solar variability impacts the results of both models. The impact of load variability seems to be minimal, indicating that the peak-preserving day-type RO is very effective. While such larger OF differences may still be tolerable given other uncertainties in Microgrid planning, they can be mitigated through hybrid optimizations (HO) that optimize technology dispatch in a second stage, using capacity results from the first stage RO and the full time-series data in the second stage. HO still supports run-time savings of 20–99%, but reduces OF differences to less than 1.5% across the board.

The choice of RO versus HO depends on individual preferences of prioritizing run-time or OF accuracy and optimized dispatch might be one of the most important features in a Microgrid Design tool since it provides the possibility to mitigate design problems and sub-optimal capacity selections. This hypothesis will be tested in follow-on research, comparing different dispatch strategies for different DER capacities in built Microgrids.

We would also like to acknowledge a limitation of this paper: the day-type approach cannot simulate energy transfer between days and months and should not be used if seasonal storage is anticipated to be part of the solution. In such cases the presented day-type MILP needs to be modified, which will be discussed in future work.

Appendix A Tariff Data

For each site, the proper utility tariff was collected or provided by the client and used in the optimization. Table A1 summarizes this information.

Table A1. Summary of electric tariffs and supporting documents.

Case	Type	State	Utility Name	Tariff Name	Source Document
Tariff Data					
Ind	Industrial/Pharmaceutical	Puerto Rico	Puerto Rico Electric Power Authority (PREPA)	LIS	[28]
Res	Residential/Public	Connecticut	Eversource Energy	Rate 56—Intermediate Time of Day	[29]
Man	Industrial/Materials	Puerto Rico	PREPA	GST	[28]
Com	Commercial/Public	Washington State	Seattle City Light	MDC—Medium General Service: city	[30]
Un1	University	Colorado	Black Hills Energy	CO935—LPS-PTOU	[31]
Un2	University	Hawai'i	HECO	HECO-P	[32]
Un3	University	California	SDGE	AL-TOU	[33]
Un4	University	Vermont	CBE	Rate 08—General Service	[34]
Mil1	Military	Texas	Confidential	Confidential	Confidential
Mil2	Military	New Mexico	Confidential	Confidential	Confidential
Mil3	Military	Maryland	Confidential	Large Power Schedule	Confidential
Mil4	Military	California	Confidential	Confidential	Confidential
Mil5	Military	Massachusetts	Confidential	Industrial Service	Confidential

Appendix B Technology Data

PV technology costs are presented in Table A2. Costs are based on client input or literature data. The PV costs include soft costs (e.g., labor costs) and inverter costs. The PV costs as well as Operation and Maintenance (O&M) costs are generally within the ranges reported by [35]. Per client request the O&M costs for Res and the PV costs for Un2 are outside of the range reported by [35].

Table A2. PV technology assumptions used in the Microgrid projects. "Max. space for PV" represents the maximum available onsite space for PV generation.

Case	PV Technology Assumptions						
	PV Costs ($/kW$_{DC}$)	O&M Costs ($/kW and Month)	Lifetime (yrs.)	Electric Efficiency (%)	Tilt (Degrees/Confidential)	Orientation (South/North, West, East, Confidential)	Max. Space for PV (m^2)
Ind	2150	0	30	16%	20	South	10,000
Res	2100	2.2	30	19%	Confidential	Confidential	3760
Man	2100	1.4	30	16%	17	South	31,876
Com	1470	0	30	16%	35	South	Unrestricted
Un1	1969	0.8	25	19%	Confidential	Confidential	Unrestricted
Un2	5000	0.8	25	15%	22	South east	20,000
Un3	1700	1.4	30	16%	Confidential	Confidential	40,000
Un4	2400	0	30	19%	30	South	41,806
Mil1	1470	1.5	20	15%	Confidential	Confidential	Unrestricted
Mil2	1470	1.5	20	15%	Confidential	Confidential	Unrestricted
Mil3	1700	1.4	20	15%	Confidential	Confidential	Unrestricted
Mil4	1700	1.4	20	15%	Confidential	Confidential	Unrestricted
Mil5	1700	1.4	20	15%	Confidential	Confidential	Unrestricted

Effective Electric Energy Storage (EES) costs and assumptions are shown in Table A3. Effective EES costs consider incentives and are, therefore, low compared to [36]. Lifetime numbers can also vary significantly depending on allowed operational conditions, meaning allowed max charging or discharging rates or minimum levels of the state of charge.

Table A4 summarizes the natural gas and diesel fired DG and CHP assets. For most cases, multiple options have been provided, mostly distinguished by different unit sizes, unit costs, electric efficiencies or the heat to power ratios. The heat to power ratio specifies the amount of heat generated from 1 kWh electricity. The data is based on vendor data and inputs from the project partners. DG and CHP capacity costs, electric efficiencies, and heat to power ratios broadly agree with the assumptions for the commercial demand model from the Annual Energy Outlook 2020 report [37]. The lifetime numbers seem to be more conservative (smaller) compared to EIA, with the exception of the microturbine lifetimes, which are higher than reported by EIA. The diesel genset costs are in line with [38].

The maximum annual operating hours are based on project constraints such as air regulation or technical constraints.

Table A3. Electric Energy Storage (EES) technology assumptions. The max. allowed charging and discharging rates are constraints within the MILP. Max allowed charge and discharge rates are defined as a function of the EES power capacity.

Case	Effective EES Costs ($/kWh)	O&M Cost ($/kW Month)	Lifetime (yrs.)	Charging/Respectively Discharge Efficiency (%)	Max. Allowed Charge Rate (-)	Max. Allowed Discharge Rate (-)	Min. SOC (-)	Max. SOC (-)	Maximum Allowed Cycles Per Year (-)	Self-Discharge Per Hour (-)
Ind	250	0	5	90%	0.3	0.3	0.3	1	n/a	0.001
Res	350	0	15	90%	0.3	1	0.1	1	n/a	0.0001
Man	500	0	20	94%	0.2	0.2	0.1	1	n/a	0
Com	350	0	20	94%	0.2	0.2	0.1	1	n/a	0.001
Un1	675	0.2	25	92%	0.3	0.3	0.1	1	110	0
Un2	566	0.2	25	90%	0.3	0.3	0.1	1	n/a	0.0001
Un3	500	0	20	94%	0.2	0.2	0.1	1	n/a	0
Un4	350	0	20	90%	0.5	0.3	0.1	1	n/a	0.0001
Mil1	212	0.3	18	87%	0.3	0.3	0	1	n/a	0.01
Mil2	212	0.3	18	87%	0.3	0.3	0	1	n/a	0.01
Mil3	212	0.3	18	87%	0.3	0.3	0	1	n/a	0.01
Mil4	212	0.3	18	87%	0.3	0.3	0	1	n/a	0.01
Mil5	212	0.3	18	87%	0.3	0.3	0	1	n/a	0.01

Table A4. Summary Fuel fired Distributed Generation (DG) and Combined Heat and Power (CHP) data.

Case	Type (/)	Unit Capacity (kW)	Lifetime (yrs.)	Capacity Costs Installed ($/kW)	O&M Fixed Costs ($/kW/year)	O&M Variable Cost ($/kWh)	Efficiency (%)	Heat to Power Ratio (%)	Max. Annual Operating Hours (hrs.)	Backup Only (Yes/No)
Ind	n/a	n/a	n/a	n/a	n/a	n/a	n/a	n/a	n/a	n/a
Res	Microturbine	60	15	3220	0.0	0.001	25%	n/a	8760	no
	Microturbine	100	15	3500	0.0	0.002	40%	n/a	8760	no
Man	CHP	3304	20	3281	0.0	0.009	24%	175%	8760	no
	CHP	3325	20	3750	0.0	0.009	44%	94%	8760	no
	CHP	5670	20	3750	0.0	0.009	28%	135%	8760	no
	CHP	7480	20	3705	0.0	0.009	45%	33%	8760	no
Com	Microturbine CHP	61	15	3220	0.0	0.013	25%	189%	8760	no
	Microturbine CHP	190	15	3150	0.0	0.016	28%	133%	8760	no
	Microturbine CHP	242	15	2700	0.0	0.012	26%	145%	8760	no
	Microturbine CHP	950	15	2500	0.0	0.012	28%	130%	8760	no
Un1	Distributed Generation	250	25	2191	0.0	0.022	23%	n/a	160	no
	Distributed Generation	250	25	2191	0.0	0.022	23%	n/a	200	no
Un2	n/a	n/a	n/a	n/a	n/a	n/a	n/a	n/a	n/a	n/a
Un3	Internal combustion engine	125	30	2000	0.0	0.020	26%	n/a	8760	no
Un4	Microturbine	100	15	2900	0.0	0.002	30%	n/a	8760	no
Mil1	Diesel genset	2000	20	600	10.0	0.000	32%	n/a	8760	yes
Mil2	Diesel genset	750	20	750	9.3	0.000	28%	n/a	8760	yes
	Diesel genset	750	20	750	9.3	0.000	28%	n/a	1091	no
Mil3	Diesel genset	750	20	750	9.3	0.000	28%	n/a	8760	yes
Mil4	Diesel genset	750	20	750	9.3	0.000	28%	n/a	8760	yes
Mil5	Diesel genset	750	20	750	9.3	0.000	28%	n/a	8760	yes

References

1. Navigant. *Microgrid Deployment Tracker 2Q18*; Navigant: Chicago, IL, USA, 2018.
2. Navigant. *Microgrid Deployment Tracker 2Q19*; Navigant: Chicago, IL, USA, 2019.
3. Wood, E. Whats Driving Microgrids toward a $30.9B Market? Microgrid Knowledge. 30 August 2018. Available online: https://microgridknowledge.com/microgrid-market-navigant/ (accessed on 4 March 2020).
4. Tozzi, P.; Jo, J.H. A comparative analysis of renewable energy simulation tools: Performance simulation model vs. system optimization. *Renew. Sustain. Energy Rev.* **2017**, *80*, 390–398. [CrossRef]
5. Lund, H.; Arler, F.; Alberg Østergaard, P.; Hvelplund, F.; Connolly, D.; Vad Mathiesenm, B.; Karnøe, P. Simulation versus Optimisation: Theoretical Positions in Energy System Modelling. *Energies* **2017**, *10*, 840. [CrossRef]
6. Fescioglu-Unver, N.; Barlas, A.; Yilmaz, D.; Demli, U.O.; Bulgan, A.C.; Karaoglu, E.C.; Atasoy, T.; Ercin, O. Resource management optimization for a smart microgrid. *J. Renew. Sustain. Energy* **2019**, *11*, 065501. [CrossRef]
7. Stadler, M.; Naslé, A. Planning and Implementation of Bankable Microgrids. *Electr. J.* **2019**, *32*, 24–29. [CrossRef]
8. REopt. Available online: https://reopt.nrel.gov/ (accessed on 4 March 2020).
9. DER-CAM. Available online: https://building-microgrid.lbl.gov/projects/der-cam/ (accessed on 4 March 2020).
10. Gabrielli, P.; Gazzani, M.; Martelli, E.; Mazzotti, M. Optimal design of multi-energy systems with seasonal storage. *Appl. Energy* **2018**, *219*, 408–424. [CrossRef]
11. Schütz, T.; Schraven, M.H.; Fuchs, M.; Remmen, P.; Müller, D. Comparison of clustering algorithms for the selection of typical demand days for energy system synthesis. *Renew. Energy* **2018**, *129*, 570–582. [CrossRef]
12. Marquant, J.F.; Mavromatidis, G.; Evins, R.; Carmeliet, J. Comparing different temporal dimensions representations in distributed energy system design models. Lausanne. *Energy Procedia* **2017**, *122*, 907–912. [CrossRef]
13. Fahy, K.; Stadler, M.; Pecenak, Z.K.; Kleissl, J. Input data reduction for microgrid sizing and energy cost modeling: Representative days and demand charges. *Renew. Sustain. Energy* **2019**, *11*, 065301. [CrossRef]
14. Bahl, B.; Kümpel, A.; Seele, H.; Lampe, M.; Bardow, A. Time-series aggregation for synthesis problems by bounding error in the objective function. *Energy* **2017**, *135*, 900–912. [CrossRef]
15. Pecenak, Z.K.; Stadler, M.; Mathiesen, P.; Fahy, K.; Kleissl, J. Robust Design of Microgrids Using a Hybrid Minimum Investment Optimization. *Appl. Energy* **2020**, *276*, 115400. [CrossRef]
16. Mashayekh, S.; Stadler, M.; Cardoso, G.; Heleno, M. A Mixed Integer Linear Programming Approach for Optimal DER Portfolio, Sizing, and Placement in Multi-Energy Microgrids. *Appl. Energy* **2017**, *167*, 154–168. [CrossRef]
17. Cardoso, G.; Stadler, M.; Mashayekh, S.; Hartvigsson, E. The impact of Ancillary Services in optimal DER investment decisions. *Energy* **2017**, *130*, 99–112. [CrossRef]
18. Milan, C.; Stadler, M.; Cardoso, G.; Mashayekh, S. Modelling of non-linear CHP efficiency curves in distributed energy systems. *Appl. Energy* **2015**, *148*, 334–347. [CrossRef]
19. Stadler, M.; Groissböck, M.; Cardoso, G.; Marnay, C. Optimizing Distributed Energy Resources and Building Retrofits with the Strategic DER-CAModel. *Appl. Energy* **2014**, *132*, 557–567. [CrossRef]
20. Cardoso, G.; Stadler, M.; Bozchalui, M.C.; Sharma, R.; Marnay, C.; Barbosa-Póvoa, A.; Ferrão, P. Optimal investment and scheduling of distributed energy resources with uncertainty in electric vehicle driving schedules. *Energy* **2014**, *64*, 17–30. [CrossRef]
21. Hanna, R.; Disfani, V.R.; Haghi, H.V.; Victor, D.G.; Kleissl, J. Improving estimates for reliability and cost in microgrid investment planning models. *J. Renew. Sustain. Energy* **2019**, *11*, 045302. [CrossRef]
22. Schittekatte, T.; Stadler, M.; Cardoso, G.; Mashayekh, S.; Sankar, N. The impact of short-term stochastic variability in solar irradiance on optimal microgrid design. *IEEE Trans. Smart Grid* **2018**, *9*, 1647–1656. [CrossRef]
23. Pecenak, Z.K.; Stadler, M.; Fahy, K. Efficient Multi-Year Economic Energy Planning in Microgrids. *Appl. Energy* **2019**, *255*, 113771. [CrossRef]
24. XENDEE. Available online: https://xendee.com (accessed on 4 March 2020).
25. OpenEI. Available online: https://openei.org/doe-opendata/dataset/commercial-and-residential-hourly-load-profiles-for-all-tmy3-locations-in-the-united-states/ (accessed on 12 February 2020).

26. Helioscope. Available online: https://www.helioscope.com/?gclid=EAIaIQobChMI8rXA-52E6AIVT_lRCh0aQwrNEAAYASAAEgJXY_D_BwE/ (accessed on 12 February 2020).

27. Dobos, A.P. *PVWatts Version 5 Manual*; NREL/TP-6A20-62641; National Renewable Energy Laboratory: Golden, CO, USA, September 2014.

28. PREPA. Available online: https://aeepr.com/es-pr/QuienesSomos/Ley57/Facturaci%C3%B3n/Tariff%20Book%20-%20Electric%20Service%20Rates%20and%20Riders%20Revised%20by%20Order%2005172019%20Approved%20by%20Order%2005282019.pdf (accessed on 27 January 2020).

29. Eversource. Available online: https://www.eversource.com/content/docs/default-source/rates-tariffs/ct-electric/rate-56-ct.pdf?sfvrsn=e941c762_32 (accessed on 22 January 2020).

30. Seattle City Light. Electric Rates and Provisions. Available online: https://www.seattle.gov/light/Rates/docs/2020/Schedule%20MDC%20Jan%201%202020.pdf (accessed on 23 January 2020).

31. Black Hills Energy. Schedule of Rates, Rules and Regulations for Electric Service. Available online: https://www.blackhillsenergy.com/sites/blackhillsenergy.com/files/coe-rates-tariff_0.pdf (accessed on 22 January 2020).

32. Maui Electric. Schedule "P" Large Power Service. Available online: https://www.mauielectric.com/documents/billing_and_payment/rates/hawaii_electric_light_rates/helco_rates_sch_p.pdf (accessed on 23 January 2020).

33. SDGE. Schedule AL-TOU. Available online: Sdge.com/sites/default/files/elec_elec-scheds_al-tou.pdf (accessed on 13 January 2020).

34. Burlington Electric. Available online: https://www.burlingtonelectric.com/rates-fees#large-general-service-lg (accessed on 13 January 2020).

35. Fu, R.; Feldman, D.J.; Margolis, R.M. *U.S. Solar Photovoltaic System Cost Benchmark: Q1 2018*; NREL/TP-6A20-72399; National Renewable National Laboratory (NREL): Golden, CO, USA, 2018.

36. Cole, W.J.; Frazier, A. *Cost Projections for Utility-Scale Battery Storage*; NREL/TP-6A20-73222; National Renewable National Laboratory (NREL): Golden, CO, USA, 2019.

37. EIA. US Energy Information Administration (EIA). Available online: https://www.eia.gov/outlooks/aeo/assumptions/pdf/commercial.pdf (accessed on 11 March 2020).

38. Ericson, S.J.; Olis, D.R. *A Comparison of Fuel Choice for Backup Generators*; National Renewable Energy Laboratory: Golden, CO, USA, 2019.